Propulsion and Power Research 2013;2(1):10–19

http://ppr.buaa.edu.cn/

Propulsion and Power Research

www.sciencedirect.com

ORGINAL ARTICLE

Time-accurate CFD conjugate analysis of transient measurements of the heat-transfer coefficient in a channel with pin fins

Tom I-P. Shih[a,*], Saiprashanth Gomatam Ramachandran[a], Minking K. Chyu[b]

[a] *School of Aeronautics and Astronautics, Purdue University, West Lafayette, IN 47907, USA*
[b] *Department of Mechanical Engineering and Material Science, University of Pittsburgh, PA 15261, USA*

Received 18 December 2012; accepted 16 January 2013
Available online 21 March 2013

KEYWORDS

Heat-transfer coefficient (HTC);
Transient technique;
Pin fins;
Time-accurate computational fluid dynamics (CFD) conjugate analysis

Abstract Heat-transfer coefficients (HTC) on surfaces exposed to convection environments are often measured by transient techniques such as thermochromic liquid crystal (TLC) or infrared thermography. In these techniques, the surface temperature is measured as a function of time, and that measurement is used with the exact solution for unsteady, zero-dimensional (0-D) or one-dimensional (1-D) heat conduction into a solid to calculate the local HTC. When using the 0-D or 1-D exact solutions, the transient techniques assume the HTC and the free-stream or bulk temperature characterizing the convection environment to be constants in addition to assuming the conduction into the solid to be 0-D or 1-D. In this study, computational fluid dynamics (CFD) conjugate analyses were performed to examine the errors that might be invoked by these assumptions for a problem, where the free-stream/bulk temperature and the heat-transfer coefficient vary appreciably along the surface and where conduction into the solid may not be 0-D or 1-D. The problem selected to assess these errors is flow and heat transfer in a channel lined with a staggered array of pin fins. This conjugate study uses three-dimensional (3-D) unsteady Reynolds-averaged Navier–Stokes (RANS) closed by the shear-stress transport (SST) turbulence model for the gas phase (wall functions

*Corresponding author.
E-mail address: tomshih@purdue.edu (Tom I-P. Shih).

Peer review under responsibility of National Laboratory for Aeronautics and Astronautics, China.

Production and hosting by Elsevier

http://dx.doi.org/10.1016/j.jppr.2013.01.003

not used) and the Fourier law for the solid phase. The errors in the transient techniques are assessed by comparing the HTC predicted by the time-accurate conjugate CFD with those predicted by the 0-D and 1-D exact solutions, where the surface temperatures needed by the exact solutions are taken from the time-accurate conjugate CFD solution. Results obtained show that the use of the 1-D exact solution for the semi-infinite wall to give reasonably accurate "transient" HTC (less than 5% relative error). Transient techniques that use the 0-D exact solution for the pin fins were found to produce large errors (up to 160% relative error) because the HTC varies appreciably about each pin fin. This study also showed that HTC measured by transient techniques could differ considerably from the HTC obtained under steady-state conditions with isothermal walls.

1. Introduction

Heat transfer plays an important role in many applications from manufacturing and materials processing to heat exchangers and thermal management. In many applications such as cooling of gas turbines and electronic components, it is important to know the temperature, the heat flux, and the heat-transfer coefficient (HTC) from surfaces exposed to convective and/or radiative environments. Considerable research has been conducted to develop techniques to enable such measurements in benign and in harsh environments (see reviews in Refs [1] and [2]). Transient techniques that use thermochromic liquid crystal and infrared imaging are widely used to measure the HTC [2–4]. With these techniques, surface temperature T_{wall} at each location is measured experimentally as a function of time. This measured temperature is then used with one of the two exact solutions to compute the HTC.

One of the exact solutions used is that for unsteady one-dimensional (1-D) conduction into a semi-infinite solid given by [5,6]

$$\frac{T_{\text{wall}}(t)-T_{\text{initial}}}{T_{\text{bulk}}-T_{\text{initial}}} = 1-\exp\left(\frac{h^2\alpha t}{k^2}\right)\operatorname{erfc}\left(\frac{h\sqrt{\alpha t}}{k}\right) \tag{1}$$

where t is time; k is the thermal conductivity of the solid; α is the thermal diffusivity of the solid; T_{initial} is temperature of the solid at $t=0$; and T_{bulk} and h are respectively the free-stream bulk temperature and the HTC, characterizing the convection environment that the solid is exposed to suddenly at $t=0$. In Eq. (1), the assumptions are k, α, h, and T_{bulk} are constants.

The other exact solution used is that for a lumped or zero-dimensional (0-D) analysis of a solid initially at T_{initial} and then suddenly at time $t=0$ is exposed to a convection environment characterized by a constant h and T_{bulk}. This exact solution, which is valid if the Biot number is much less than 0.1, is given by [5]

$$\frac{T_{\text{wall}}(t)-T_{\text{bulk}}}{T_{\text{initial}}-T_{\text{bulk}}} = \exp\left[-\left(\frac{hA_{\text{s}}}{\rho V C_{\text{p}}}\right)t\right] \tag{2}$$

where A_{s} is the area of the solid's surface that is exposed to the convection environment; V is the volume of the solid; ρ is density; and C_{p} is the constant-pressure-specific heat. All other parameters have the same definition as those in Eq. (1).

As noted, Eqs. (1) and (2) involve a number of assumptions. Of these, the most critical is the assumption that h and T_{bulk} are constants because it is generally not the case in practice. Also, for Eq. (1), the assumption of 1-D conduction is suspect for problems with complicated geometries. Thus, the objective of this study is twofold. The first is to examine the implications of the assumptions in Eqs. (1) and (2) when used with transient measurements of the HTC. The second is to examine whether the HTC obtained by a transient technique will be the same as the HTC obtained at steady-state conditions with isothermal wall boundary conditions.

This study is accomplished via computational fluid dynamics (CFD) conjugate analysis based on both steady and unsteady Reynolds-averaged Navier–Stokes (RANS) for a problem in which the free-stream/bulk temperature T_{bulk} and the heat-transfer coefficient h vary appreciably along the surface and where conduction into the solid may not be 0-D or 1-D. The problem selected is flow and heat transfer in a channel lined with a staggered array of pin fins.

The organization of the rest of this paper is as follows. First, the problem studied is described. This is followed by the formulation of the problem, the numerical method of solution, and the computational approach to achieve the objectives of this study. Afterwards, the results of this study are presented.

2. Description of test problem

The problem studied is shown in Figure 1 (not drawn to scale). All dimensions in this figure are given in terms of the diameter of the pin fin, which is $D=12.5$ mm. As shown in the figure, the problem consists of a channel of length $L_2+L_3+L_4=20D+25D+48D$ and

Nomenclature

h	heat transfer coefficient (HTC), $h=q''/(T_{bulk}-T_{wall})$
H	height of duct
k	thermal conductivity
L_3	length of the test section with the pin fins
L_1, L_2, L_4	length of channel upstream and downstream of test section
Nu	Nusselt number, $Nu=hD_h/k$
p	pressure
q''_{wall}	heat flux at the wall
T, T_{bulk}	temperature, bulk temperature
T_{in}	temperature at the duct inlet
T_{wall}	wall temperature
U_{in}	mean velocity at the duct inlet
X	coordinate in the streamwise direction
y^+	$y^+=\rho U_\tau y/\mu$, where y is the normal distance from the wall and $U_\tau=(\tau_w/\rho)^{0.5}$
Y	coordinate in the spanwise direction
Z	coordinate in the direction aligned with the axis of the pin fins

Greek letters

ε	dissipation rate of turbulent kinetic energy
μ	dynamic viscosity
ρ	density
τ_w	wall shear stress

height $2H=2.25D$ bounded by two plates of thickness $2D$. Within this channel are 11 rows of pin fins located between $X=0$ and $X=L_3$ that are arranged in a staggered fashion. The spacing between adjacent pin-fin centers is $P=2.5D$ in the X-direction and $W=1.5D$ in the Z-direction. For the two plates that form the channel from $X=-L_2$ to $X=L_3+L_4$, the surfaces at $Y=H+2D$ and $Y=-(H+2D)$ are maintained adiabatic. The portion of the channel from $X=-(L_1+L_2)$ and $X=-L_2$, where $L_1=200D$, has adiabatic walls so that the thermal boundary layer in the channel will not start until $X=-L_2$. Because of the symmetry of this problem, only the domain bounded by $X=-(L_1+L_2)$ and $X=L_3+L_4$, $Y=0$ and $Y=H+2D$, and $Z=0$ and $Z=W$ is considered in the analysis.

For this channel with pin fins, the fluid that enters the channel is air. The plates that bound the channel are made of plexiglass, and the pin fins in the channel are made of aluminum. Plexiglass was selected as the material for the channel plate so that the heat conduction into the plate will be nearly one-dimensional (1-D) and occur slowly so that it will take relatively long time before the heat conduction could penetrate across the plexiglass plate. Aluminum was selected as the material for the pin fin so that heat conduction into the pin fin is so fast that the temperature evolution within the pin could be approximately zero-dimensional (0-D) or lumped, which will be the case if the Biot number is small (e.g., much less than 0.1). These are typical of the materials used by experimentalists when implementing transient methods for measuring HTC. In this study, the properties of the plexiglass and aluminum were assumed to be constants. For the plexiglass, the thermal conductivity k, the constant pressure specific heat C_p, the density ρ, and the thermal diffusivity α are taken to be 0.2085 W/(m · K), 1466 J/(kg · K), 1185 kg/m^3, and 1.2×10^{-7} m^2/s, respectively. For the aluminum, k is 202.4 W/(m · K), C_p is 871 J/(kg · K), ρ is 2719 kg/m^3, and α is 8.5464×10^{-5} m^2/s.

On operating conditions, there are two types—a time-accurate version to study the assumptions invoked in the transient measurement techniques and a steady-state version to study the connection between transient measurements of the HTC and steady-state values of the HTC with isothermal walls. For both operating conditions, air with uniform temperature T_{in} of 350 K and uniform velocity U_{in} of 20 m/s in the X-direction enters the channel at $X=-(L_1+L_2)$, and the static pressure at the exit of the channel p_b is set at 1 bar (100 kPa). For the time-accurate version, the temperature of the air and in all solids (plate and pin fins) was initially at $T_{initial}=300$ K. For the steady-state version, the temperature of the plate wall at $Y=H$ and between $X=-L_2$ and $X=L_3+L_4$ was maintained at $T_{wall}=340$ K.

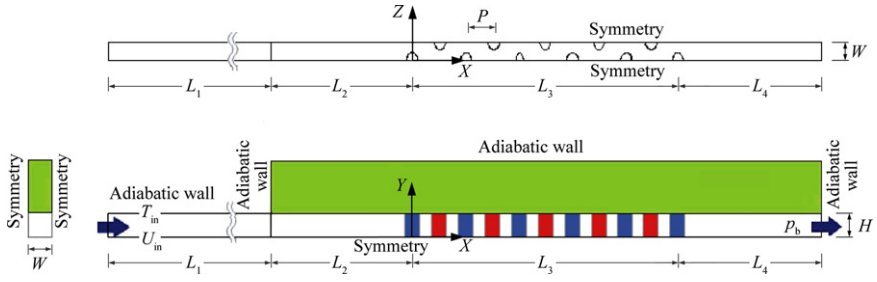

Figure 1 Schematic of the problem studied.

The surfaces of all pin fins were also maintained at $T_{wall}=340$ K.

3. Formulation of problem, numerical method of solution, and approach to assess errors

In this study, the governing equations used for the gas phase are the unsteady form of the ensemble-averaged continuity, compressible Navier–Stokes, and energy equations for a thermally perfect gas with the Sutherland model for the viscosity and temperature-dependent properties. The effects of turbulence were modeled by the shear-stress transport (SST) model of Mentor [7]. For the solid phase in the conjugate analysis, the Fourier law was used.

Solutions to the governing equations were obtained by using the ANSYS Fluent Version 13.0 code [8]. Both time-accurate and steady-state solutions were obtained. When time-accurate solutions were of interest, the implicit coupled scheme with second-order accuracy in time was employed, and 30 iterations per time step were used to achieve convergence at each time step. This number of iteration was determined by numerical experiments. When steady-state solutions were sought, the SIMPLE (semi-implicit method for pressure-linked equations) segregated scheme was used for the gas phase until convergence is achieved. For both steady and time-accurate solutions, the fluxes for all equations at the cell faces were interpolated by using the second-order upwind scheme. Pressure equation and the Laplace equation for the conduction were also computed by using second-order accuracy.

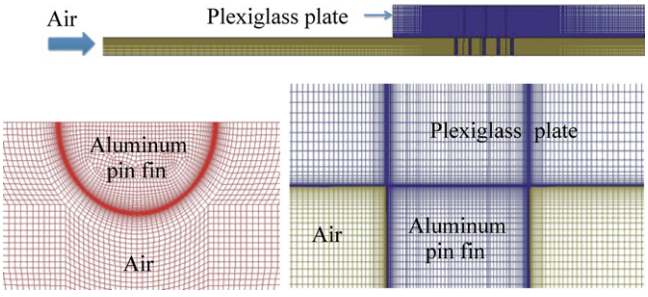

Figure 2 The grid system used.

Figure 2 shows the grid system employed. The total number of cells used is 4,139,030. The number of cells in the channel is 1501 along the X-direction, 35 along the Y-direction, and 38 along the Z-direction from $X=-L_2$ onwards and 16 cells in Z-direction upstream of $X=-L_2$. The number of cell about 180 degrees of the pin fin in the azimuthal direction is 111. Inside each half pin fin, the number of cells is 54,460. In the plate, the total number of cells is 1,893,430 with 1422 in the X-direction, 35 in the Y-direction, 38 in the Z-direction. As shown in the figure, cells are also clustered about the air–wall interface. This is to capture the low-Reynolds-number region of the turbulent flow next to the wall, where y^+ of cells next to walls were less than unity. The cluster next to the air–wall interface on the solid side is to resolve the penetration of the conduction heat transfer into the plate and the pin fin with very small time-step sizes. The grid was arrived at via a grid sensitivity study.

For time-accurate CFD conjugate analysis, the solution procedure is implemented in the following order:

(1) Set initial temperature everywhere (air, plexiglass, and pin fins) at $T_{initial}=350$ K (instead of 300 K).
(2) Obtain steady-state solution with $T_{in}=350$ K; $U_{in}=20$ m/s; and $p_b=1$ bar (100 kPa). Since $T_{in}=T_{initial}$, the temperature field remains essentially uniform since viscous dissipation is negligible.
(3) Reset the temperature in all solids (plexiglass and pin fins) at $T_{initial}=300$ K.
(4) At time $t=0$, start time accurate simulations.

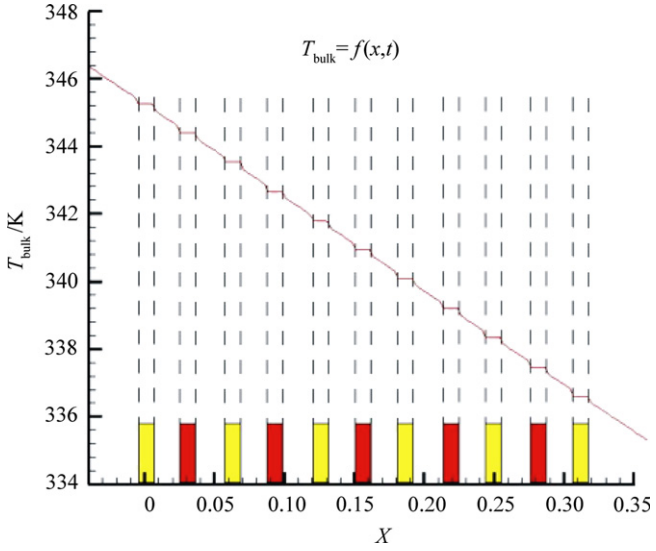

Figure 3 The interpolation of the bulk temperature is linear between rows of pin fins and constant within each row of pin fins.

The time-step sizes Δt employed were as follows. For the first 1500 time steps, $\Delta t = 1 \times 10^{-5}$ seconds. Then, it was ramped up steadily to 1×10^{-3} seconds and held there.

(5) At any time t, the bulk temperature T_{bulk} is computed by linearly interpolating from the bulk temperature at $X = -8D$ to $X = L_3 + 8D$ at that instant of time, where T_{bulk} is taken to be constant along X wherever there is a row of pin fin present as shown in Figure 3.

(6) The HTC at any location and any instant of time is computed by

$$h = q''_{wall}/(T_{bulk} - T_{wall}) \quad (3)$$

where q''_{wall}, T_{bulk}, and T_{wall} are the wall heat flux, bulk temperature, and wall temperature respectively at time t.

For steady-state solutions, h is also given by Eq. (3) except q''_{wall} and T_{bulk} are time independent and vary only with position with $T_{wall} = 340$ K.

Note that in transient measurement techniques, T_{wall} is measured and then inserted into Eq. (1) or (2) to get h. In this computational study, T_{wall} is computed by the time-accurate conjugate CFD analysis and then inserted into Eq. (1) or (2) to get h. Since the h computed by using Eq. (3) does not invoke any of the assumptions employed in Eq. (1) and Eq. (2), the h computed by Eq. (3) could be used to assess the accuracy of the h computed by using Eq. (1) for the surface of the flat plate at $Y = H$ and the h computed by using Eq. (2) for the pin-fin surface. In this comparison between the h obtained by Eq. (3) and Eq. (1) or Eq. (2), $T_{initial}$, T_{bulk}, and T_{wall} are the same.

4. Results

The results of this study are organized to examine the following three questions:

- What is the error invoked by using Eq. (1) when measuring the HTC?
- What is the error invoked by using Eq. (2) when measuring HTC?
- Is transient measurement/computation of HTC the same as steady-state measurement/computation of the HTC?

4.1. Error invoked by using Eq. (1)

Figure 4 shows the HTC computed by using Eq. (3) and Eq. (1) as a function of time at $X = -8D$, $Y = H$, and $Z = W/2$ on the surface of the plexiglass plate. From this figure, it can be seen that as time progresses, the HTC given by the 1-D solution denoted as h-1D approaches the correct HTC given by Eq. (3) denoted as h-CFD. This excellent agreement is expected since far upstream of the pin fins, the assumptions invoked by Eq. (1) are sound approximations. This excellent agreement is also a check on the unsteady CFD conjugate analysis and in the algorithm used to solve for the HTC in Eq. (1). However, it is interesting to note that h-1D and h-CFD do not equal the HTC computed by CFD at steady-state conditions with isothermal walls, a subject that will be discussed in Section 4.3.

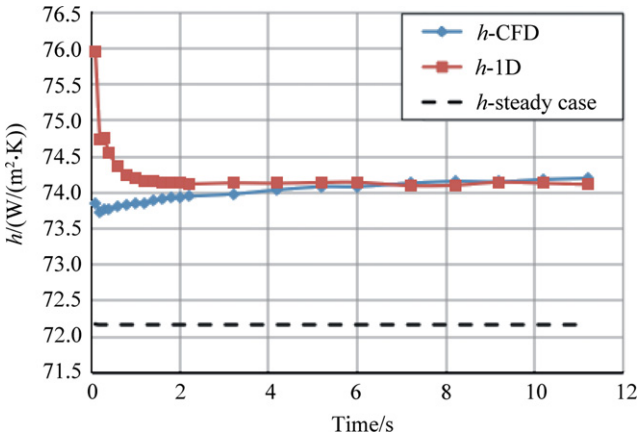

Figure 4 Heat-transfer coefficient predicted by Eq. (3) denoted as h-CFD & h-steady-state vs. that predicted by Eq. (1) denoted as h-1D on the plate at $X = -8D$, $Y = H$, and $Z = W/2$.

Figures 5 to 7 show the HTC computed by using Eqs. (1) and (3) as a function of time at several locations on the surface of the plexiglass plate—just upstream of the first, third, fourth, and fifth pin fin, denoted as p1a, p3a, p4a, and p5a, respectively; near the side of the first, second, third, fourth, and fifth pin fin, denoted as p1b, p2b, p3b, p4b, and p5b, respectively; and just downstream of the first, third, fourth, and fifth pin fin, denoted as p1c, p3c, p4c, and p5c, respectively. From Figure 5, it can be seen that h-CFD is always higher than h-1D just upstream of the pin fins except near the beginning ($t < 4$ seconds). Also, h-CFD appears to plateau as time advances, but h-1D does not. As a result, the difference between h-CFD and h-1D increases with time. Figure 6 shows the evolution of h-CFD and h-1D with time at points just downstream of the pin fins to be quite different from those just upstream of pin fins. Except for the first pin, h-1D is larger than h-CFD for the first eight to ten seconds. Afterwards, h-CFD becomes larger than h-1D. Figure 7 shows the evolution of h with time for locations next to pin fins, and they are similar to those at locations just upstream of pin fins. These differences show the effects of the multi-dimensional conduction in the solid and the spatial variations of the HTC and the bulk temperature.

In thermochromic-liquid-crystal measurements of the HTC, only the temperature 37.6 °C is measured because it emits the highest intensity radiation (green light) and so could be detected most accurately. Thus, the time t at which every point on the surface reaches 37.6 °C is recorded. Then, Eq. (1) uses the T_{bulk} at that time

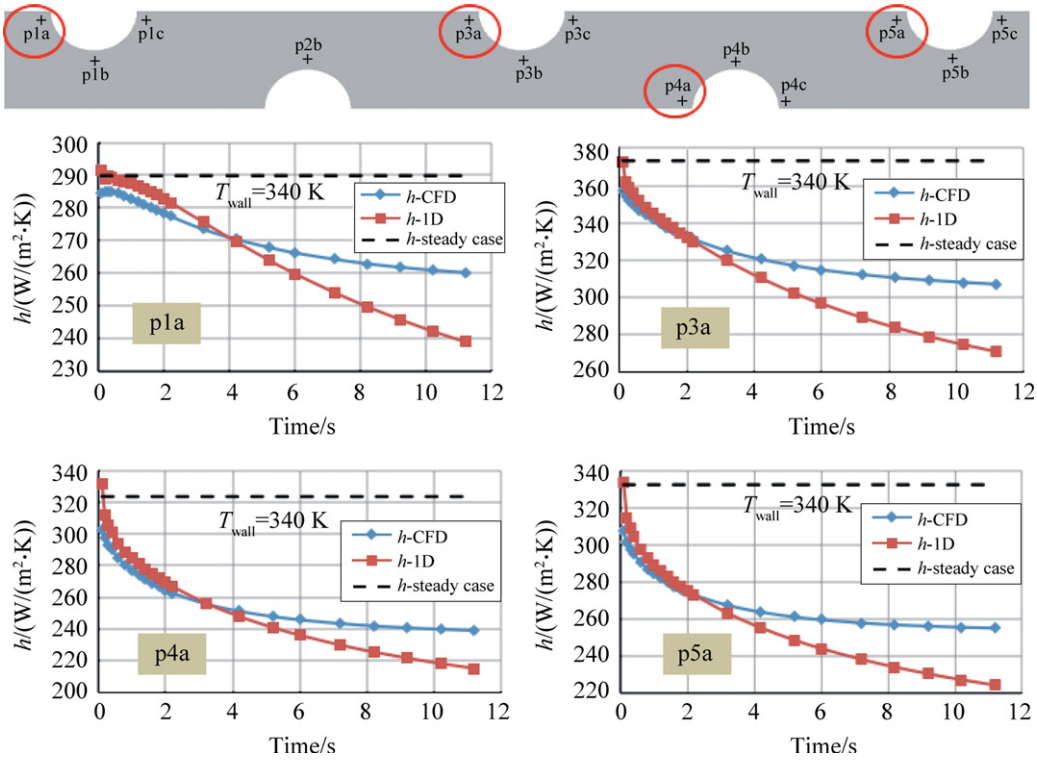

Figure 5 Heat-transfer coefficient predicted by Eq. (3) denoted as *h*-CFD & *h*-steady-state vs. that predicted by Eq. (1) denoted as *h*-1D on the plexiglass plate at locations just upstream pin fins.

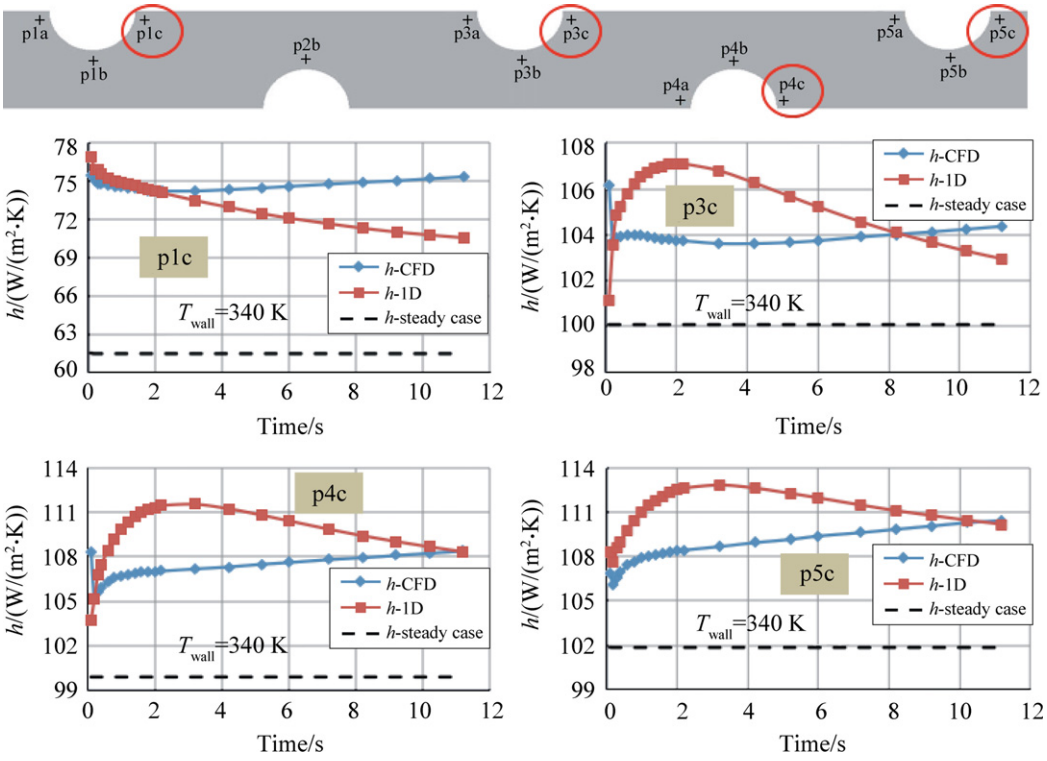

Figure 6 Heat-transfer coefficient predicted by Eq. (3) denoted as *h*-CFD & *h*-steady-state vs. that predicted by Eq. (1) denoted as *h*-1D on the plexiglass plate at locations just downstream pin fins.

along with with $T_{wall}=37.6\ ^{\circ}C$ to compute *h*-1D. Figure 8 shows the relative error in *h*-1D thus computed by comparing with *h*-CFD computed at that same time when $T=37.6\ ^{\circ}C$. From Figure 8, it can be seen that the error created by Eq. (1) is less than 5% for the conditions of the present study. Though less than a

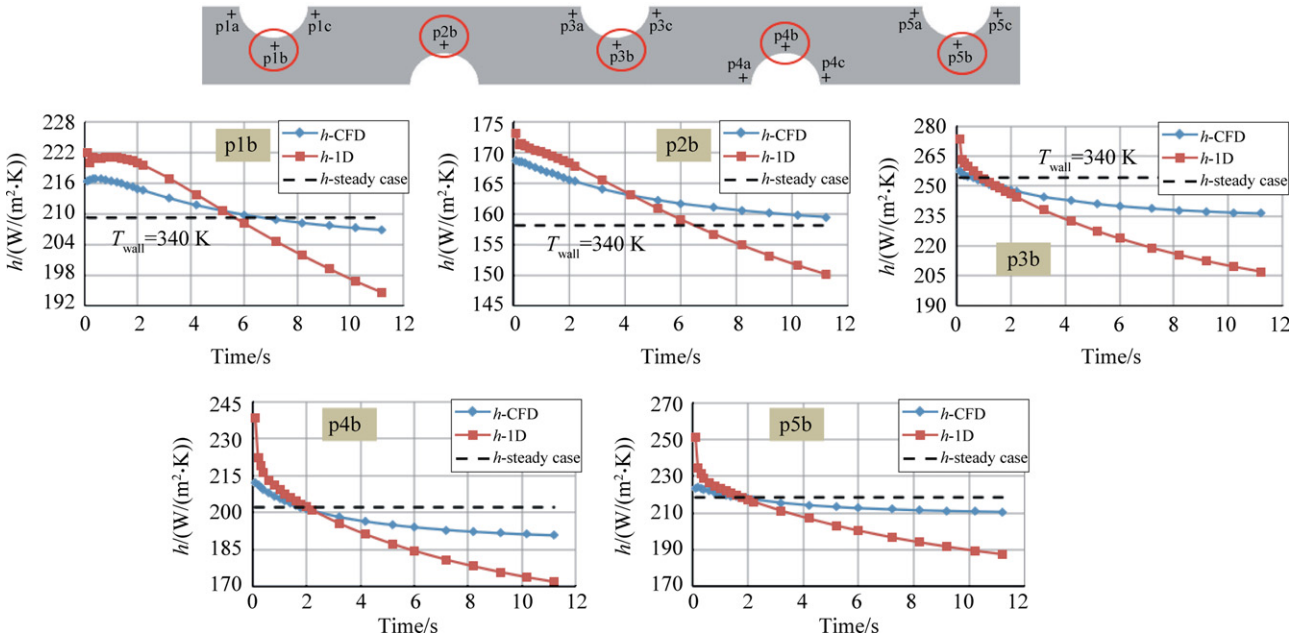

Figure 7 Heat-transfer coefficient predicted by Eq. (3) denoted as h-CFD & h-steady-state vs. that predicted by Eq. (1) denoted as h-1D on the plexiglass plate at locations just on the side of pin fins.

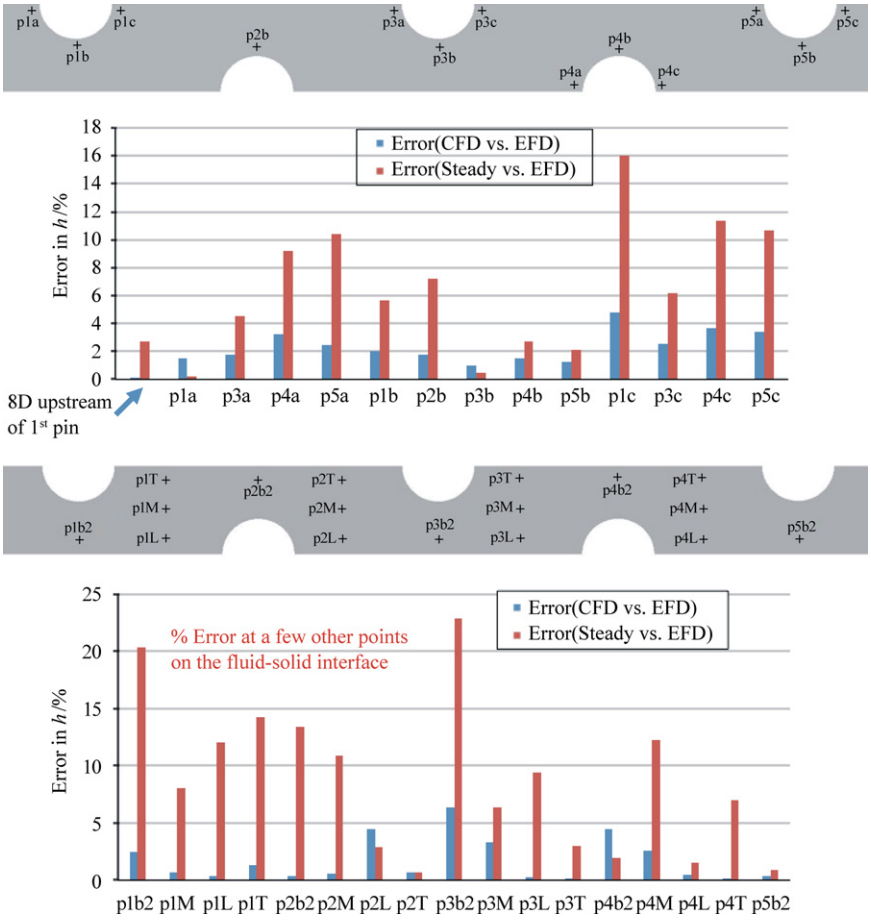

Figure 8 Relative error between h-CFD and h-1D at selected points.

5% relative error may be acceptable, it is important to note that the HTC measured/computed is generated under unsteady conditions, where the wall temperature is constantly changing. Thus, the question that remains is: Are transient measurements/computations of HTC representative of HTC under steady-state conditions? The answer to this question is addressed in Section 4.3.

4.2. Error invoked by using Eq. (2)

Figure 9 shows the temperature in the pin fin at time $t=2.2$ seconds computed by the time-accurate CFD conjugate analysis. From this figure, it can be seen that the temperature distribution in the pin fin is nearly uniform ($<1\,^{\circ}C$ difference throughout). This is expected since the Biot number for the pin fins is extremely small ($\ll 0.1$). Thus, the 0-D assumption for the pin fin is quite good. However, though the temperature inside each pin fin is nearly uniform at each instant of time, Figure 9 shows the HTC given by h-CFD to vary considerably about the surface of each pin fin. This large variation in HTC is expected since the flow around each pin fin is quite complicated with flow impinging on the pin fin's leading edge, horseshoe vortex at the pin-fin/plate junction, and wake behind each pin fin. Each of these flow structures produces very different local HTC.

Figure 10 shows the HTC predicted by Eq. (2) and denoted by h-0D. From this figure, it can be seen that h-0D at selected points on the pin fin surface all approach some common value on the order around 150 $W/(m^2 \cdot K)$. However, this value differs considerably from h-CFD at the same selected points on the pin-fin surface. The relative error in h-0D could be as much as 200%. Thus, Eq. (2) produces very poor results. This is because Eq. (2) assumes the HTC to be the same about the entire pin fin, and for the problem studied, this is simply not true. Thus, Eq. (2) must be used carefully. Not only the Biot number must be less than 0.1, the HTC must also be nearly the same about the entire object being lumped.

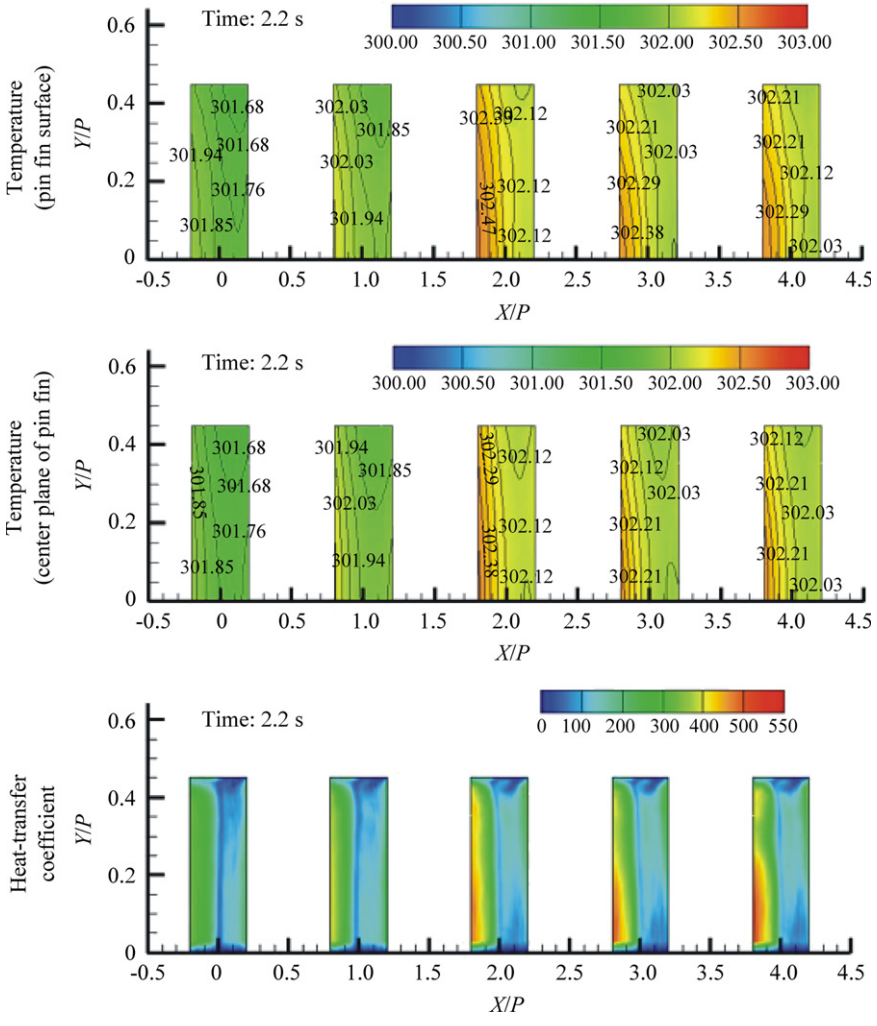

Figure 9 Temperature and heat-transfer coefficient for pin fins at $t=2.2$ seconds.

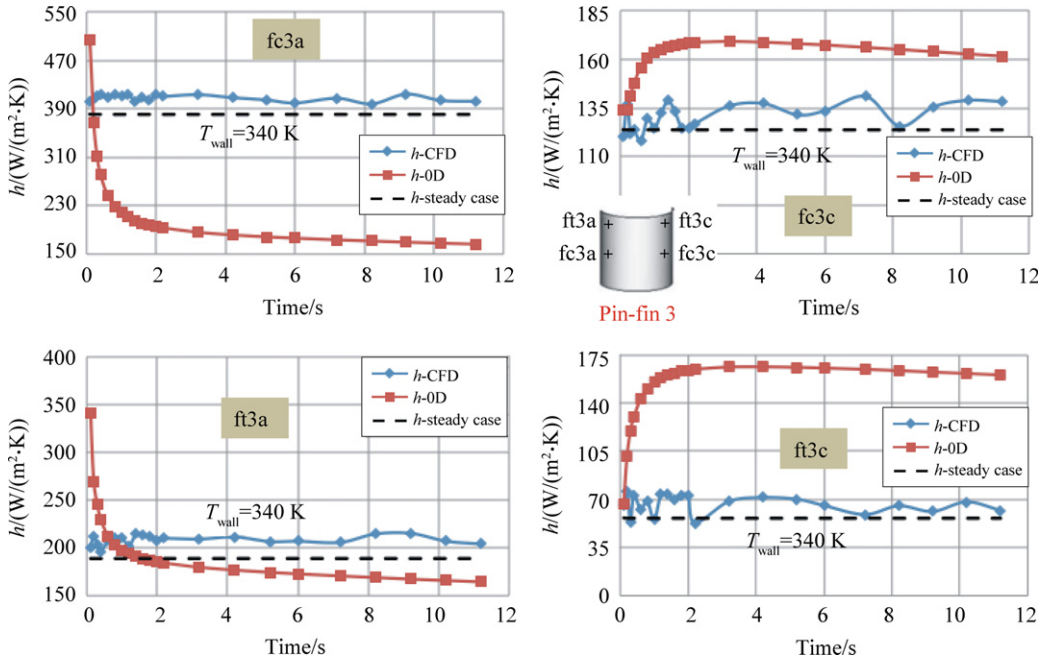

Figure 10 Relative error between *h*-CFD and *h*-1D at selected points.

4.3. Transient measurement/computation of h vs. steady-state measurement/computation of h

Figures 5 to 7 show transient measurements/computations of the HTC do not match the steady-state measurements/computations of the HTC. Figure 8 shows the error in *h*-1D relative to *h*-CFD-steady on the plate surface to be as high as 11% just upstream of pin fins, 16% just downstream of pin fins, and 23% on the plate between pin fins. From Figure 5 to 8, it can be shown that the HTC obtained from time-accurate CFD conjugate analysis at the time when $T=37.6\ ^{\circ}C$ can have a relative error as high as 20%–30% when compared to the HTC obtained from steady-state CFD analysis with isothermal-wall boundary conditions. This error occurs because the HTC of compressible flows is a strong function of the wall temperature, and for transient methods, the temperature on the wall is constantly changing. Since transient measurements of the HTC are often used to guide the design of steady-state devices and to validate results from steady RANS with isothermal wall boundary conditions, this question on whether transient measurements/computations of the HTC is meaningful under steady-state conditions needs further investigation. In the above discussion, the wall temperature for the steady-state simulations was set at 340 K = 67 °C, which is considerably higher than 37.6 °C, the temperature at which the HTC was measured by the experiment. If the temperature of the isothermal wall was set at 37.6 °C for the steady-state simulations, then the HTC from the steady and the unsteady simulations do match better.

5. Conclusion

Time-accurate CFD conjugate analyses were performed to examine possible errors in transient techniques used to measure the heat-transfer coefficients. For the conditions of the present study (flow and heat transfer in a channel with pin fins), it was shown that transient techniques that use the unsteady, 1-D exact solution for the semi-infinite wall to give reasonably accurate "transient" heat-transfer coefficients on the wall (<5% relative error). Transient techniques that use the exact solution of the lump analysis, however, were shown to give heat-transfer coefficients with considerable error for the pin fins (up to 160% relative error). This is because for each pin fin, though the temperature distribution can be lumped, the heat-transfer coefficient varies greatly. This study also showed that the heat-transfer coefficient obtained under transient conditions, where the wall temperature is changing with time, could differ considerably from those obtained under steady-state conditions with isothermal walls. This error could be reduced if the steady-state simulation sets the temperature of the isothermal equal to the temperature at which the heat-transfer coefficient is measured, which is 37.6 °C for the present problem.

Acknowledgments

This research was supported by the National Energy Technology Laboratory of the US Department of Energy with Robin Ames and Richard Dennis as the technical monitors. The authors are grateful for this support.

References

[1] E.R. Eckert, R.J. Goldstein, Measurements in Heat Transfer, 2nd edition, Hemisphere Publishing Corp., Washington, 1976.

[2] J.C. Han, S. Dutta, S.V. Ekkad, Gas Turbine Heat Transfer and Cooling Technology, Taylor & Francis, New York, 2000 (Chapter 6).

[3] C. Camci, K. Kim, S.A. Hippensteele, A new hue capturing techniquefor the quantitative interpretation of liquid crystal images used in convective heat transfer studies, ASME Journal of Turbomachinery 114 (4) (1992) 765–775.

[4] M.K. Chyu, H. Ding, J.P. Downs, F.O. Soechting, Determination of local heat transfer coefficient based on bulk mean temperature using a transient liquid crystal technique, Experimental Thermal and Fluid Science 18 (2) (1998) 142–149.

[5] F.P. Incropera, D.P. De Witt, Fundamentals of Heat and Mass Transfer, 5th edition, John Wiley and Sons, New York, 2002.

[6] J.V. Beck, C.R. Claire St., B. Blackwell, Inverse Heat Conduction, John Wiley and Sons, New York, 2008.

[7] F.R. Menter, Two-equation eddy-viscosity turbulence models for engineering applications, AIAA Journal 32 (8) (1994) 1598–1605.

[8] ANSYS, Inc. http://www.ansys.com/Products/Simulation+Technology/Fluid+Dynamics/ANSYS+Fluent.